# Quasi-Particle Self-Consistent *GW* for Molecules

F. Kaplan,[†] M. E. Harding,[†] C. Seiler,[‡] F. Weigend,[‡,§] F. Evers,[‡] and M. J. van Setten[*,¶]

[†]Institute of Nanotechnology, Karlsruhe Institute of Technology, Campus North, D-76344 Karlsruhe, Germany

[‡]Institute of Theoretical Physics, University of Regensburg, D-93040 Regensburg, Germany

[¶]Nanoscopic Physics, Institute of Condensed Matter and Nanosciences, Université Catholique de Louvain, 1348 Louvain-la-Neuve, Belgium

[§]Institute of Physical Chemistry, Karlsruhe Institute of Technology, Campus South, D-76021 Karlsruhe, Germany

Ⓢ *Supporting Information*

ABSTRACT: We present the formalism and implementation of quasi-particle self-consistent *GW* (qs*GW*) and eigenvalue only quasi-particle self-consistent *GW* (ev*GW*) adapted to standard quantum chemistry packages. Our implementation is benchmarked against high-level quantum chemistry computations (coupled-cluster theory) and experimental results using a representative set of molecules. Furthermore, we compare the qs*GW* approach for five molecules relevant for organic photovoltaics to self-consistent *GW* results (sc*GW*) and analyze the effects of the self-consistency on the ground state density by comparing calculated dipole moments to their experimental values. We show that qs*GW* makes a significant improvement over conventional G_0W_0 and that partially self-consistent flavors (in particular ev*GW*) can be excellent alternatives.
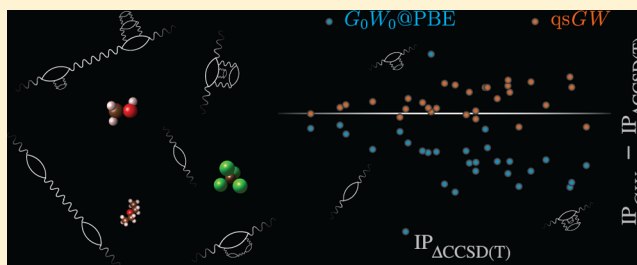
1. INTRODUCTION

The sufficiently accurate prediction of photoionization processes is still a serious computational challenge. The main workhorse for medium and large sized systems is the Kohn–Sham density functional theory (KS-DFT).[1,2] As is very well-known, using KS-DFT eigenvalues (especially using semilocal functionals) for computational spectroscopy has, however, various fundamental and practical limitations. Moreover ΔSCF ionization energies, which are more accurate, are in general only applicable to obtain the first ionization energies.[3−5] An approach promising better accuracy for the calculation of single particle excitations is the *GW*-method. Its central object is the Green's function G.[6−9] It is calculated by solving the Dyson equation that relates the full (interacting) Green's function to a known noninteracting reference one, G_0, via a self-energy Σ. Depending on the starting point, G_0, Σ adds or corrects exchange and (dynamical) correlation. In *GW* theory Σ is approximated evaluating the Fock diagram, however employing a screened interaction W. Since the Green's function, G, exhibits (complex) poles that describe the (charged) excitation energies (and their lifetimes),[10,11] *GW* theory represents a simple and transparent framework for the investigation of ionization processes.

Since *GW* comes with a substantial computational effort, a great variety of simplified flavors of *GW* are in use, the most common being so-called G_0W_0 approximation.[9] It treats the self-energy Σ as a first order (i.e., nonselfconsistent) perturbation acting on a KS or Hartree–Fock (HF) reference system. It produces sizable corrections, in particular to the energies of the frontier orbitals, at moderate computational cost; thus medium sized molecules can be treated efficiently. These advantages are reflected in an increasing number of applications in quantum chemistry.[12−50]

However, the lack of self-consistency in G_0W_0 implicates undesirable shortcomings: Both, G and the polarization P, that enter the calculation are imported without change from the underlying reference calculation (KS or HF). As a consequence, G_0W_0 depends on the choice of the reference systems, e.g., the exchange-correlation (XC) functional of KS-DFT calculation. Furthermore, there is no update in the spatial shape of the orbitals, so the ground state density of G_0W_0 reproduces the one of the reference theory.

These limitations are overcome by imposing self-consistency. However, due to the fact that fully self-consistent *GW* (sc*GW*) is computationally expensive,[25,34,51−59] it is highly desirable to explore the potential of partially self-consistent schemes. In this work we follow a procedure toward partial self-consistency that is numerically still tractable and gives promising results: the quasi-particle (QP) self-consistent *GW* (qs*GW*). For solids there is already encouraging experience with this approach,[60−67] and first applications to atoms[36] and small molecules[59] also seem promising. Here it is adapted for use in a general quantum chemistry code. Our results indicate that the starting point dependence, observed at the G_0W_0 level, which can easily exceed 1.0 eV,[25,38,40,52,59,68−75] is completely removed in qs*GW*.

Our calculations suggest that the effects of orbital updates can be often neglected in comparison to the correction coming from the shifts in the pole positions of the Green's function. Therefore, we also implement and investigate a simplified version of qsGW in which the orbitals are kept fixed at the reference (DFT of HF) result, and only the QP-energies are updated (eigenvalue only GW, evGW). Also this and similar schemes have been successful already in implementations for solids[76−78] and first applications in molecular geometries.[26,41,49] It is an approximation especially beneficial for larger systems since it is computationally less demanding than scGW (and qsGW). An important aspect of our work is that we present a systematic comparison between qsGW and evGW providing a validation of evGW. In particular we find that in evGW the starting point dependence is strongly reduced as compared to G_0W_0.

An important aspect of testing a new methodology is comparison with other approaches. A generally popular reference are experimental values. This commonly adopted practice can however be misleading in the case of ionization energies. One difficulty is that the experimental ionization energies are often adiabatic, whereas those calculated within the GW scheme are always vertical. In addition intrinsic effects originating from zero-point vibrations and relativistic effects (beyond those that enter via the reference calculation) are usually not included and are also not in our current approach. (We mention that at the G_0W_0 level a two component extension has been implemented recently to account for spin−orbit effect for closed shell molecules.[47]) Therefore, a comparison to more accurate theoretical results would be more reliable. In this work, we make use of the possibility to compare our results to coupled-cluster singles and doubles augmented by a perturbative treatment of triple excitations (CCSD(T))[79,80] employing the same atomic structure and basis set.[81] Doing so rules out experimental uncertainties, temperature and zero-point renormalization effects, etc., but also basis set errors to a large part.

Our paper is organized as follows: In section 2.1 we present the formalism that is used within our implementation of qsGW. Section 2.2 explains the details of the implementation. The third section validates the qsGW method. First, our implementation is tested for internal consistency (section 3.1), i.e. we test the convergence behavior with the basis set and the number of iteration cycles. Second, the qsGW method is assessed using first ionization potentials (IP) of a set of 29 representative molecules (section 3.2).[40,52] Third, we compare higher IPs with experimental data (section 3.3) and with results using the scGW implementation within the FHI-AIMS software package[52] (section 3.3). Furthermore, we evaluate the ground state densities and the dipole moments in section 3.5. In section 4 we compare the results of qsGW to those of G_0W_0.

In section 5 we investigate two different approaches of partial self-consistency. We first introduce and benchmark our implementation of the evGW method (self-consistency in the poles positions of G and the response function) versus qsGW and CCSD(T). In section 5.2 we test the $G_{ev}W_0$[49] approach (self-consistent only in the poles positions of G) versus qsGW. Finally section 6 contains an analysis of the computational performance and scaling behavior of the presented methods.

2. METHOD

2.1. qsGW Approximation.
We are aiming at an approximate self-consistent solution of the Dyson equation

$$G(E) = (E - H[G] - \Sigma[G])^{-1} \tag{1}$$

Here, $H[G]$ denotes the Hartree contribution incorporating the external potential (respectively the ions), the kinetic contribution, and the Hartree potential. The latter depends on the charge density and hence is considered as a functional of G.

In the GW-approximation[9] the self-energy is given in terms of the causal Green's function

$$\Sigma(\mathbf{r}, \mathbf{r}', \omega) = \frac{i}{2\pi} \int d\omega' G(\mathbf{r}, \mathbf{r}', \omega + \omega') W(\mathbf{r}, \mathbf{r}', \omega') e^{i\eta\omega'} \tag{2}$$

and the screened Coulomb interaction W. η denotes a positive infinitesimal. W is obtained from the following equation

$$W(\mathbf{r}, \mathbf{r}', \omega) = v(\mathbf{r}, \mathbf{r}') + \int d\mathbf{r}'' \int d\mathbf{r}''' v(\mathbf{r}, \mathbf{r}'') P(\mathbf{r}'', \mathbf{r}''', \omega) W(\mathbf{r}''', \mathbf{r}', \omega) \tag{3}$$

with $v(\mathbf{r}, \mathbf{r}') = e^2 |\mathbf{r} - \mathbf{r}'|^{-1}$ denoting the bare Coulomb kernel. Ignoring vertex corrections (consistent with the construction of Σ) the polarization P is calculated within the random phase approximation (RPA)

$$P_{RPA}(\mathbf{r}, \mathbf{r}', \omega) = -\frac{i}{2\pi} \int d\omega' G(\mathbf{r}, \mathbf{r}', \omega + \omega') G(\mathbf{r}, \mathbf{r}', \omega') e^{i\eta\omega'} \tag{4}$$

2.1.1. Quasi-Particle Equation and Quasistatic Approximation. A solution of eq 1 is constructed by introducing a quasi-spectral representation

$$G(\mathbf{r}, \mathbf{r}', z) = \sum_n \frac{\psi_{r,n}(\mathbf{r}, z) \bar{\psi}_{l,n}(\mathbf{r}', z)}{z - \varepsilon_n(z) + i\eta \operatorname{sgn}(\varepsilon_n(z) - \mu)} \tag{5}$$

The right and left eigenvectors, $\psi_{r,n}(\mathbf{r}, z)$, $\psi_{l,n}(\mathbf{r}, z)$, and eigenvalues $\varepsilon_n(z)$ represent quasi-particle/hole (QP/QH) states and energies, μ being the chemical potential. The bar in $\bar{\psi}_{l,n}(\mathbf{r}', z)$ denotes the complex conjugate. The (complex) poles z of the Green's function 5 follow from the pole condition

$$z - \varepsilon_n(z) = 0 \tag{6}$$

The QP-orbitals as well as the energies are found as solutions of the QP-equations

$$(\varepsilon_n(z) - H_H[G] - \Sigma[G]) \cdot \psi_{r,n}(\mathbf{r}, z) = 0 \tag{7}$$

$$\psi_{l,n}(\mathbf{r}, z) \cdot (\varepsilon_n(z) - H_H[G] - \Sigma[G]) = 0 \tag{8}$$

Within qsGW the self-energy 2 is approximated by an energy-independent, Hermitian matrix. In the literature different variants have been proposed for such approximate self-energies.[61,62,82] Here we follow Faleev et al.[61]

$$\bar{\Sigma}_{nn'} = \frac{1}{2} (\Sigma_{nn'}(\varepsilon_n) + \Sigma_{nn'}(\varepsilon_{n'})) \tag{9}$$

This approximation takes into account the quasi-particle part of the Green's function and neglects lifetime effects. One of its merits is that it implies a consistent treatment of the renormalization factor Z within the calculation of many observables.[61]

Removing the energy dependence from the self-energy has important computational benefits. First, the energy integration in eq 2 can be performed analytically. Second, the approximate self-energy takes a Hermitian form hence left and right eigenvectors coincide

$$(\varepsilon_n - H_H[G] - \tilde{\Sigma}[G]) \cdot \psi_n(\mathbf{r}) = 0 \tag{10}$$

and the poles are real, reflecting an effective single particle theory. Consequently, the Green's function of qsGW takes the form

$$G(\mathbf{r}, \mathbf{r}', E) = \sum_n \frac{\psi_n(\mathbf{r})\bar{\psi}_n(\mathbf{r}')}{E - \varepsilon_n + i\eta\,\mathrm{sgn}(\varepsilon_n - \eta)} \tag{11}$$

2.1.2. Kohn–Sham Initialization. An iterative procedure of solving eqs 10 and 11 self-consistently is typically initialized with a KS Green's function constructed from the KS orbitals $\psi_n^{(0)}(\mathbf{r})$ and energies $\varepsilon_n^{(0)}$

$$G^{(0)}(\mathbf{r}, \mathbf{r}', E) = \sum_n \frac{\psi_n^{(0)}(\mathbf{r})\bar{\psi}_n^{(0)}(\mathbf{r}')}{E - \varepsilon_n^{(0)} + i\eta\,\mathrm{sgn}(\varepsilon_n^{(0)} - \eta)} \tag{12}$$

2.2. Implementation. qsGW has been implemented within a local version of the TURBOMOLE package, building on the routines for the calculation of the G_0W_0 self-energy.[40]

The solution of eq 10 is organized in an iterative scheme starting from the KS-initialization eq 12. The QP-orbitals of the $(i+1)$th iteration $\psi_n^{(i+1)}(\mathbf{r})$ are expressed in the reference orbitals of the previous iteration

$$\psi_n^{(i+1)}(\mathbf{r}) = \sum_{\underline{n}} \mathcal{A}_{n\underline{n}}^{(i+1)} \psi_{\underline{n}}^{(i)}(\mathbf{r}) \tag{13}$$

In the reference basis $\psi_{\underline{n}}^{(i)}(\mathbf{r})$ eq 10 takes the form of an eigenvalue problem

$$\sum_{\underline{n}} \mathcal{A}_{n'\underline{n}}^{(i+1)} \left[\int d\mathbf{r}' \int d\mathbf{r}\ \psi_n^{(i)}(\mathbf{r})(H_H[G^{(i)}]\delta(\mathbf{r} - \mathbf{r}') \right.$$
$$\left. + \tilde{\Sigma}(\mathbf{r}, \mathbf{r}'))\psi_{\underline{n}}^{(i)}(\mathbf{r}') \right] = \varepsilon_{n'}^{(i+1)} \mathcal{A}_{n'n}^{(i+1)} \tag{14}$$

The diagonalization of eq 14 yields updates in $\varepsilon_{n'}^{(i+1)}$ and $\mathcal{A}_{n'n}^{(i+1)}$. With the latter new orbitals $\psi_n^{(i+1)}(\mathbf{r})$ are constructed via 13. These are orthonormal by construction due to the hermiticity of the operators in eq 14.

Since hermiticity gives the present scheme a form similar to an effective single particle problem we can take advantage of established (DFT) routines to calculate the Hartree Hamiltonian $H_H[n^{(i+1)}]$, $n^{(i+1)} = \sum_{i=1}^N |\psi^{(i+1)}{}_n(\mathbf{r})|^2$ employing an updated density.

For the computation of the matrix elements of the self-energy

$$\Sigma_{n\underline{n}}(E) = \langle n|\Sigma_x|\underline{n}\rangle + \langle n|\Sigma_c(E)|\underline{n}\rangle \tag{15}$$

we recall the expressions already derived before in the context of the G_0W_0 implementation.[40] The expression for the real part of a matrix element of the correlation part Σ_c of the self-energy reads

$$\mathrm{Re}(\langle n|\Sigma_c(E)|n'\rangle) = \sum_m \left[\sum_i^{occ} (in|\rho_m)(\rho_m|n'i) \right.$$
$$\times \frac{E - \varepsilon_i + \Omega_m}{(E - \varepsilon_i + \Omega_m)^2 + \bar{\eta}^2} + \sum_a^{unocc} (an|\rho_m)(\rho_m|n'a)$$
$$\left. \times \frac{E - \varepsilon_a - \Omega_m}{(E - \varepsilon_a - \Omega_m)^2 + \bar{\eta}^2} \right] \tag{16}$$

where ρ_m and Ω_m denote the two particle excitation densities and energies, and $\bar{\eta}$ is a positive infinitesimal. To express the exchange part we employ the common notation of the Coulomb integrals

$$(pq|rs) = \int d\mathbf{r} \int d\mathbf{r}' p(\mathbf{r})q(\mathbf{r}) \frac{1}{|\mathbf{r} - \mathbf{r}'|} r(\mathbf{r}')s(\mathbf{r}') \tag{17}$$

$p(\mathbf{r})$, $q(\mathbf{r})$, etc. denoting single particle orbitals, e.g. of QP or KS type.

The unscreened exchange part of qsGW is identical to the exchange contribution of HF theory

$$\langle n|\Sigma_x|n'\rangle = \sum_{\underline{n}}^{occ} (n\underline{n}|\underline{n}n') \tag{18}$$

where the sum is over all occupied (QP-)orbitals.

Employing the quasi-spectral representation, eq 5, the new self-energy is calculated from the updated pole positions $\varepsilon_{n'}^{(i+1)}$ and orbitals $\psi_n^{(i+1)}(\mathbf{r})$. This uses the established routines from the G_0W_0 implementation, taking into account all changes, i.e. in both G and W.

After the approximation eq 9 is applied, the next iteration is started by solving again eq 14. This procedure is continued until a self-consistent solution is achieved.

2.2.1. Convergence Criteria. In terminating the self-consistency cycle different convergence criteria are conceivable. An obvious choice would consider the change of the QP energies from one cycle to the next. However, motivated by earlier work,[52] we check for the norm of the differences of the Green's functions

$$\Delta = \frac{1}{N_{Orbitals}^2} \sum_{n,\underline{n}} |G_{n\underline{n}}(E = 0) - G_{n\underline{n}}^{(i-1)}(E = 0)| \tag{19}$$

$$= \frac{1}{N_{Orbitals}^2} \sum_n |G_{nn}(E = 0) - G_{nn}^{(i-1)}(E = 0)| \tag{20}$$

The last step is valid when $G_{n\underline{n}}$ is diagonal, i.e. given in the orthonormal eigenstates of the QP-equation. Typically the iteration is stopped if $\Delta < 10^{-7}$ is achieved. This corresponds to orbital energies being converged to within 1 meV.

2.2.2. Linear Mixing. The iterative approach introduced above does not always converge into a fixed point solution. To improve stability and also rate of convergence we introduce a linear mixing scheme that mixes into the updated Green's function a contribution of the previous one to decrease the step width between two iterations in a similar manner as done for iterative procedures for the HF or DFT ground state. Therefore, strictly speaking we do not solve eq 14, but

$$[\varepsilon_n^{(i+1)} - (\lambda(H_H[G^{(i)}] + \Sigma[G^{(i)}]) + (1 - \lambda)\varepsilon_n^{(i)})]\psi_n^{(i+1)} = 0 \tag{21}$$

Our tests indicate that $\lambda = 0.3$ is a reasonable choice which converges all studied molecules and, on average, speeds up the convergence by factor 4 as compared to no mixing. As an example Figure 1 shows the convergence using different mixing parameters for BF.

3. VALIDATION OF qsGW

In this section we will first confirm the internal consistency of the implemented qsGW method. Second, we will benchmark, for a test set of 29 representative molecules, qsGW versus ΔCCSD(T) first IPs and experimental results of higher IPs of 5
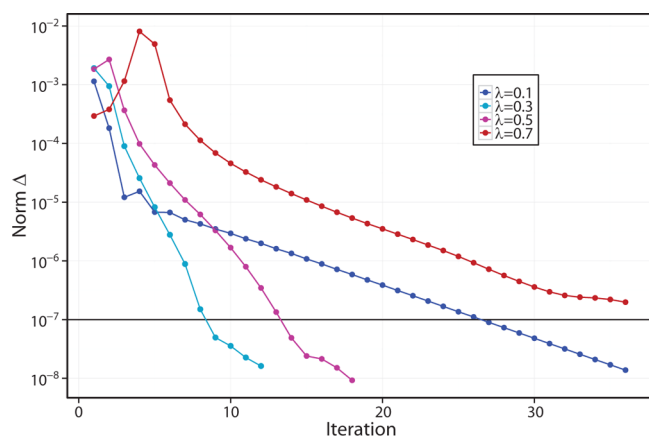
Figure 1. Flow of the convergence of the norm of the difference of the Green's functions from two iterations with the qsGW iteration for the BF. The termination criterion is indicated by the solid line.

organic molecules. Finally the results of qsGW are compared to full self-consistency GW (scGW) literature results to validate the accuracy of qsGW and to shed light on the internal features of the quasi-static approximation.

3.1. qsGW Internal Consistency. We investigate the basis set dependence of the implemented qsGW method and extract a basis set which yields a good trade-off of computational cost and accuracy. Furthermore, we will show that the results of qsGW are independent of the chosen initial functional in the initializing calculation.

3.1.1. Basis Set Convergence. We start the study of the basis set dependence of the qsGW IPs by a comparison for three small molecules, water, nitrogen, and methane. The results obtained using the def2-SVP, def2-TZVP, def2-TZVPP, and def2-QZVP basis set series are shown in Figure 2.[83,84] The results are plotted against the inverse of the size of the basis set. We take the ordinate offset of the linear extrapolation (the dashed lines in Figure 2) of the def2-TZVP and def2-QZVP as an estimate for the extrapolated complete basis set limit (CBS) result. This same approach has been used and tested in two of
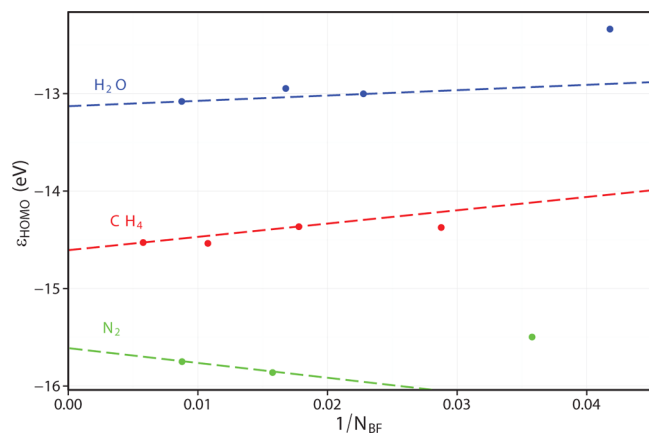
Figure 2. Convergence test of the qsGW-ionization potential with respect to the basis set (using, from left to right, the def2-QZVP, def2-TZVPP, def2-TZVP, and def2-SVP basis sets) of water, nitrogen, and methane. For the nitrogen dimer def2-TZVP and def2-TZVPP are identical. The intersection of the linear extrapolation of the def2-TZVP and def2-QZVP points with the ordinate gives an estimate for the complete basis set limit (CBS).

our previous studies for G_0W_0 comparing also to other basis sets.[40,48] In these studies it turned out to have an estimated error typically within 50 meV for G_0W_0. Since the same physical quantities enter in qsGW as in G_0W_0, it is reasonable to assume that the same holds for qsGW as well. Indeed for these three molecules we observe the same rate of convergence as for G_0W_0.[40] We therefore use this approach also for qsGW, at least as long as thoroughly tested extrapolation schemes as known for Hartree−Fock or coupled-cluster energies are not available.

In a similar manner as shown in Figure 2, we have performed a survey over a larger subset of our test set of molecules and calculated the CBS limit for each individual molecule; the overall convergence behavior is indicated in Figure 3. For the
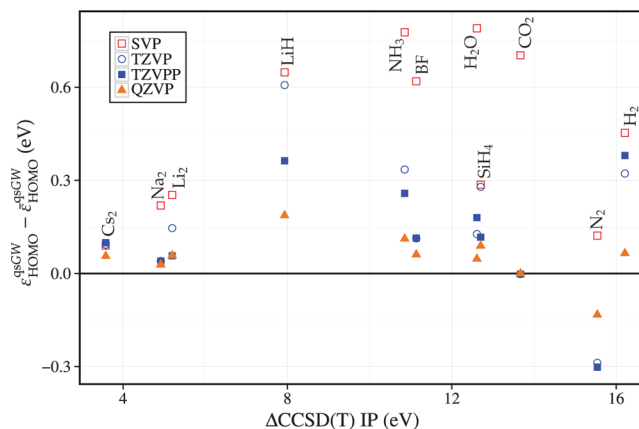

Figure 3. Change of the qsGW-ionization potential ϵ with increasing size of the basis set (using the def2-SVP, def2-TZVP, def2-TZVPP, and def2-QZVP basis sets)[83,84] using the complet basis set limit (CBS) $\bar{\epsilon}$ as reference. The CBS is obtained from a linear interpolation over the inverse of the number of basis functions, see also Figure 2.

def2-SVP basis set we find a maximum error larger than 0.8 eV. Furthermore, the largest deviations are seen for systems with strong polar covalent bonds (H_2O, LiH, and NH_3). (This has already been observed for G_0W_0 in ref 40). Our interpretation is that the def2-SVP basis set is not flexible enough to describe the high charge accumulation at one of the bond partners in ionic bonding situations. Therefore, the def2-SVP results have been excluded from the procedure to obtain the CBS limit.

Overall we find that the def2-TZVP basis shows a maximal deviation of roughly 0.4 eV. With the higher polarized def2-TZVPP basis set, for most molecules the deviation drops below 0.3 eV. Previously we have shown that for larger molecules the error actually is smaller.[48] Beyond def2-TZVP the quality of the GW results mainly depends on the total number of basis functions, not necessarily the quality of the basis functions at the individual atoms. Moreover, the CCSD(T) results are available in the def2-TZVPP basis set, making those the ideal candidate for an accurate and unbiased comparison. We hence take the def2-TZVPP basis set as a reasonable compromise for the current study, with an uncertainty due to the basis set of maximally a few hundred meV. For highly accurate calculations def2-QZVP basis sets are however recommended. Using these for self-consistent calculations routinely, however, requires further parallelization of the response and GW routines in TURBOMOLE.

3.1.2. Starting Point Dependence. A major advantage of self-consistent GW schemes is that the fixed-point found in the iteration scheme is for the commonly used starting points

(largely) independent of the initialization.[85] This is true also for qsGW, as is illustrated in Figure 4. The convergence of the
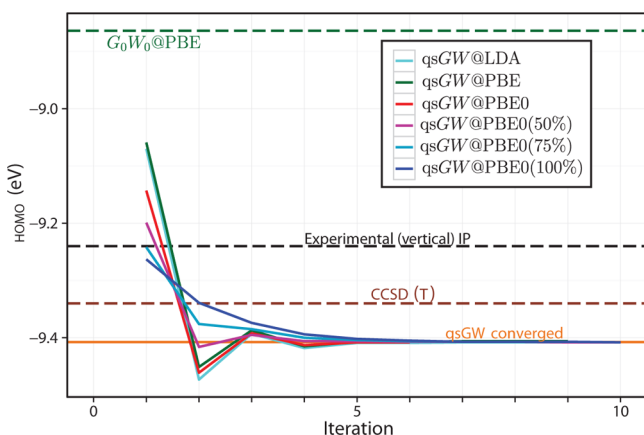
Figure 4. Convergence of the HOMO energy for benzene with the qsGW iterative cycle using the def2-TZVPP basis set. In this example the self-consistency cycle was initialized with a KS-DFT Green's function calculated employing LDA, PBE, and PBE hybrid XC-functionals with an exact exchange contribution of 25% (PBE0), 50%, 75%, and 100%. For comparison also the G_0W_0, the experimental, and ΔCCSD(T)[81] results are shown.

HOMO energy with increasing cycle number starting from different Kohn−Sham XC-functionals is shown for the example of benzene. In this work we explore the LDA,[86] PBE,[87] PBE0,[88] and PBE0(X%) (PBE0 with X % exact exchange). The iterative procedure converges into exactly the same solution, independent of the starting point.

3.2. First Ionization Potential: Comparison to ΔCCSD-(T). As a first quantitative test we calculate the ionization energies/potentials (IP) for a test set of 29 molecules ranging from H_2 to tetrathiafulvalene.[89] We focus on IPs since (i) they are an important indicator to understand charge transfer processes, (ii) experimental reference data is available, and (iii) one has access to results using more accurate theories (at least for small size molecules). The first IP is trivially extracted from the calculated data being the (negative) energy of the highest occupied molecular orbital (HOMO). These and all following results have been calculated using the def2-TZVPP basis set.[83,84]

The G_0W_0 results have been calculated initialized from DFT using the PBE functional, denoted G_0W_0@PBE. In the calculation of the correlation part of the self-energy the positive infinitesimal η was chosen so that all (orbital-)energies are converged within 1 meV. Typically $\eta = 1$ meV was used. For all calculations the RI approximation was used. It has been shown previously that the errors introduced by RI, applying the standard auxiliary basis functions,[84] are, except for very small systems like He, Ne, and H_2, below 100 meV.[48] The parameters for the qsGW calculations were chosen to converge the pole-positions within 1 meV.

The obtained IPs are compared to results obtained by employing the coupled-cluster method in the CCSD(T) approximation,[81] using the same atomic structures and same basis set as were used in the GW calculations (def2-TZVPP).

The deviations in the calculated HOMO energies using the different flavors of GW to ΔCCSD(T) IPs are displayed in Figure 5. Together with the experimental (vertical) IPs the calculated IPs are reported in Table 1. The data shows an
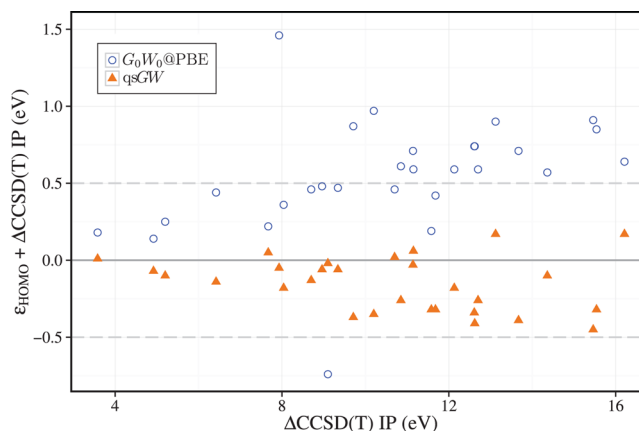
Figure 5. Deviations of the HOMO energies using G_0W_0@PBE and qsGW with IPs from ΔCCSD(T)[81] calculations. The corresponding numerial data is provided in Table 1, and statistical evaluation of the deviations is shown in Table 2.

Table 1. Calculated (Minus) HOMO Energies from qsGW and G_0W_0 (Initialized from DFT Employing the PBE Functional Using the def2-TZVPP Basis Set) as well as Experimental (Vertical) Ionization Potentials and Estimates from ΔCCSD(T)[81][b]

molecule	exp.	ΔCCSD(T)[81]	G_0W_0	qsGW
H_2	15.42	16.21	15.57	16.04
Li_2	5.11	5.20	4.95	5.30
Na_2	4.89	4.92	4.78	4.99
Cs_2	3.70	3.58	3.40	3.57
F_2	15.70	15.46	14.55	15.91
N_2	15.58	15.54	14.69	15.86
BF	11.00	11.14	10.43	11.17
LiH	7.90	7.93	6.47	7.98
CO_2	13.78	13.67	12.96	14.06
H_2O	12.62	12.61	11.87	12.95
NH_3	10.85	10.85	10.24	11.11
SiH_4	12.82	12.70	12.11	12.96
SF_4	12.30	12.62	11.88	13.03
Au_2	9.50	9.10	9.84	9.12
Au_4	8.60	7.67	7.45	7.62
methane	14.35	14.36	13.79	14.46
ethane	12.00	13.12	12.22	12.95
propane	11.51	12.13	11.54	12.31
butane	11.09	11.58	11.39	11.90
isobutane	11.13	11.68	11.26	12.00
ethylene	10.68	10.70	10.24	10.68
acetone	9.70	9.71	8.84	10.08
acrolein	10.11	10.20	9.23	10.55
benzene	9.24	9.34	8.87	9.40
naphthalene	8.09	8.04	7.68	8.22
thiophene	8.85	8.96[a]	8.48	9.02
benzothiazole	8.75	8.70[a]	8.24	8.83
1,2,5-thiadiazole	10.11	10.09[a]	9.65	10.18
tetrathiofulvalene	6.72	6.42[a]	5.98	6.56

[a]This work. [b]All values are in eV, and all calculated results are obtained with the def2-TZVPP basis set.

improved agreement of qsGW with ΔCCSD(T) in comparison to the G_0W_0@PBE results, by up to 1.41 eV. The mean absolute error (MAE) improves by 0.40 eV, see Table 2, from the single-shot G_0W_0 to the self-consistent qsGW estimates.

Furthermore, the increasing trend in the discrepancy is cleared within qsGW.

Table 2. Statistical Measures of the Difference of the Calculated IP from G_0W_0 and qsGW to the reference ΔCCSD(T) IP Accumulated over the Test Set[a]
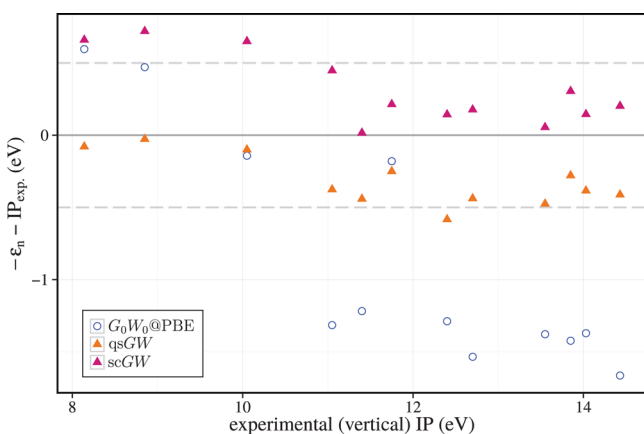
	G_0W_0	qsGW
ME	0.57	−0.16
MAE	0.59	0.19
σ^2	0.08	0.02
MaxAE	1.49	0.45
MinAE	0.14	0.01

[a]All values are in eV.

3.3. Higher Ionization Potentials: Comparison to scGW and Experiment.

In this section we discuss the accuracy of qsGW for the calculation of higher IPs. The higher IPs are difficult to access via CCSD(T). For the first ionization energy the total energy difference between the neutral and cationic ground state has to be calculated. Calculating the latter correctly is already delicate. For the higher ionization energies excited states of the cation have to be calculated. This makes these calculations very cumbersome (sometimes impossible). We therefore fall back to experimental values as references.[90]

We extended our test with five organic molecules that are candidates for optical devices and for which also experimental data is available. These molecules have already been investigated with scGW by Caruso et al.[52,57] We will compare the G_0W_0, qsGW, and scGW spectra to experimental results. The results are shown for naphthalene in this section; the results on three more molecules (thiophene, benzothiazole, and 1,2,5-thiadiazole) are available in the Supporting Information.

In Figure 6 higher IPs using G_0W_0 and qsGW as well as scGW are compared to the experimental (vertical) IPs for

Figure 6. Deviation of the QP-energies between G_0W_0, qsGW, and scGW[52] (FHI-AIMS) from experimental ionization energies for naphthalene. The dashed line indicates the deviation of ±0.5 eV.

naphthalene. The G_0W_0 and qsGW methods show similar behavior as described in the previous section. Furthermore, IPs from qsGW and scGW give similar agreement with experiment. qsGW clearly outperforms scGW for the lowest ionization energies, but for the higher ionization energies scGW becomes better. Both self-consistent methods, qsGW and scGW, remove most of the energy dependence in the error of G_0W_0. Actually, we find a rigid shift of about 0.5 eV for all energy levels between

qsGW and scGW for nearly all molecules investigated. A similar picture is observed for the three further molecules where we compare the higher ionization energies between qs and scGW (see the Supporting Information). For these rather similar aromatic systems we observe in all cases a shift ~0.5 eV. Whether this holds for a broader class of molecules needs further systematic investigation, especially since the molecules in this comparison exhibit very similar bonding situations.

The shift can be understood by recalling the split of the Green's function into a quasi-particle part and an incoherent part

$$G = ZG^{QP} + \overline{G} \qquad (22)$$

In qsGW the Z-factor is unity and the incoherent part $\overline{G}$ is neglected, while in the scGW both are taken into account. We suggest that $\overline{G}$ is only weakly energy dependent, so that its contribution $\overline{\Sigma} = i\overline{G}W$ to the self-energy is also a relatively flat function of energy. The current data, and the results by Koval et al.,[59] show that for molecules the effect of the quasi particle approximation however has the opposite sign as in solids. Vanschilfgaarde and co-workers argue that calculating the response from the full green function, as in scGW, would lead to underscreening and hence overestimation of the ionization energies.[62] This is indeed what one would conclude from results on the homogeneous electron gas.[91] In the present results on molecules scGW underestimates and qsGW overestimates. A systematic study aiming to understand this inversion including many more molecules, exhibiting different kinds of bonding, is currently in progress.

3.4. Comparison to qsGW Literature Results.

Recently Koval et al. also compared qsGW and scGW for a set of molecules.[59] Their work employs a spectral function technique on an equidistant energy grid to calculate the convolution of G and W. Their method 'A' is the same as the approach used in this work, Bruneval's implementation in molgw,[36] and the original implementation by Faleev et al.[61] for solids.[92]

To make a definite test for the agreement between the three different implementations of qsGW for molecules, we calculate the helium atom using the basis set employed in the works by Koval et al. and Bruneval, the correlation-consistent basis sets.[93] The results are compared in Table 3. We observe an excellent

**Table 3. HOMO Energies for Atomic Helium from qsGW, Literature Comparison[a]**

basis	qsGW B[59]	qsGW A[59]	qsGW[36]	qsGW (this work)
cc-pVDZ	24.346	24.350	24.359	24.359
cc-pVTZ	24.554	24.340	24.320	24.320
cc-pVQZ	24.668	24.751	24.766	24.767
cc-pV5Z	24.705	24.799	24.825	24.826

[a]All values are in eV.

agreement with Brunevals results at the meV level. In contrast, we observe a deviation to the 'A' method of Koval et al. that is quite substantial, in the tens of meV range. For comparison Table 3 also lists the results from the approximate 'B' method.

3.5. Densities and Dipole Moments.

A self-consistent solution of the GW equations introduces corrections in the spatial shape of the QP-orbitals in addition to shifts of the pole positions of the Green's function. Hence, corrections to the ground state density as compared to the reference density can arise.

Figure 7 shows the differences between the calculated electron densities of benzene for DFT(PBE), DFT(PBE0), and
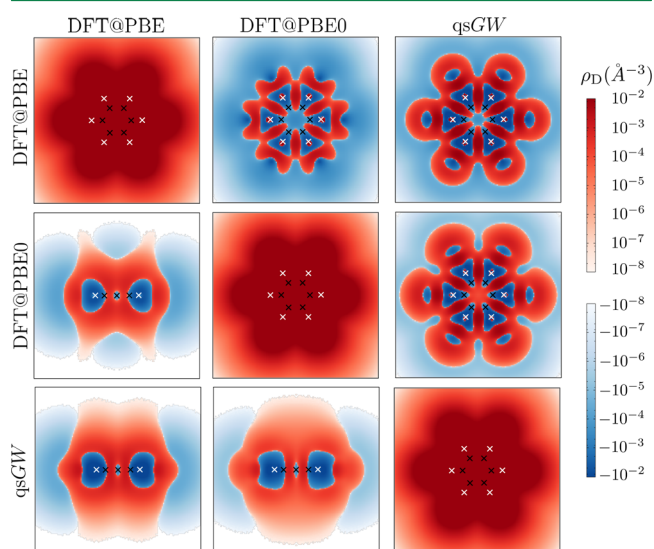
Figure 7. Diagonal: Ground state electron density of benzene as obtained from DFT(PBE), DFT(PBE0), and qsGW. Off-diagonal upper right: Difference in the ground state electron densities: PBE−PBE0, PBE-qsGW, and PBE0-qsGW, horizontal cut. Off-diagonal lower left: Same differences, vertical cut. The positions of the atoms are indicated by the black (carbon) and white (hydrogen) crosses. The results from the qsGW calculation show a slightly stronger localized density (blue area) around the H−C pairs in comparison to the DFT(PBE) calculations.

qsGW, showing that the qsGW orbitals are slightly more localized. This localization is caused by the cancelation of a large part of the spurious self-interaction of the approximate DFT functionals. The part of the self-interaction that is caused by self-screening is not canceled in qsGW.[94] Removing this as well would require the inclusion of more diagrams.[95]

The enhanced tendency toward localization displays clearer looking at an ionic molecule like HF, see Figure 8; we observe a more localized density around the fluoride atom. Furthermore, the amount of charge on the nonbonding side of the hydrogen
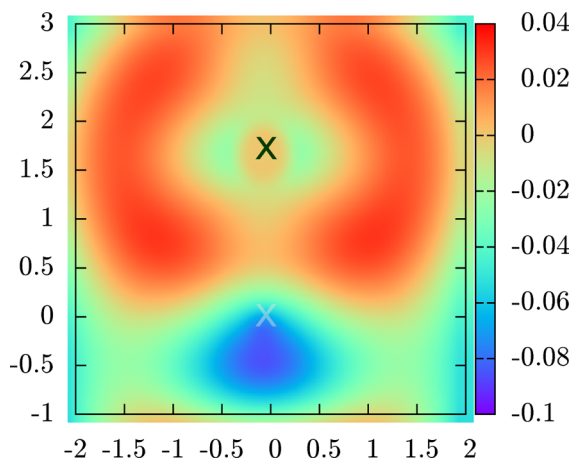
Figure 8. Difference between the calculated DFT (PBE) density and the qsGW density normalized on the (initial) DFT density for hydrogen flouride. The fluoride atom is denoted by a green cross; the hydrogen atom is denoted by a gray cross.

atom is slightly reduced. The trend seen here for qsGW agrees with the observations of Caruso et al. for scGW.[57]

An experimentally easily accessible observable characterizing the ground state density is the dipole moment. The comparison is given in Table 4. To also be able to compare to scGW we will present here the systems used by Caruso et al.

Table 4. Comparison between Experimental[97] and Theoretical Dipole Moments (Debye), from PBE, PBE0, PBE0(75%), PBE0(100%), HF, scGW[52] (FHI-AIMS), and qsGW[a]

	LiH	HF	LiF	CO	ME	MAE
exp.	5.88	1.82	6.28	0.11		
PBE	5.60	1.80	5.99	0.24	−0.12	0.18
PBE0(25%)	5.77	1.85	6.18	0.11	−0.05	0.06
PBE0(75%)	6.01	1.93	6.45	0.14	0.11	0.11
PBE0(100%)	6.10	1.97	6.54	0.26	0.20	0.20
HF	6.03	1.95	6.50	0.26	0.16	0.16
scGW[52]	5.9	1.85	6.48	0.07	0.05	0.07
qsGW	5.83	1.84	6.29	0.07	−0.02	0.03

[a]For all calculations the experimental equilibrium bond length was considered, and the calculations of this work are performed in the def2-TZVPP basis set.

While HF typically overestimates the dipole moment of these molecules, DFT typically slightly underestimates it. In the range of hybrid functionals the most accurate dipole moments are obtained from the PBE0 functional. scGW performs comparable to PBE0. In contrast, qsGW yields better agreement with an overall mean absolute error (MAE) of 0.03 D. To make a definitive statistically sound statement discriminating between the qsGW and scGW is however not possible due to the small number of systems. In conclusion, our results support the general impression that self-consistent GW is a promising tool to investigate the charge-transfer in molecular interfaces and other (nanoscale) heterostructures.[96]

Comparing the differences between sc and qs GW for on one hand the ionization energies and on the other hand the dipole moments, we observe a different degree of agreement. The dipole moments tend to agree better between the two methods than the ionization energies. We assume this to be related to the rigid shift we observed between two respective spectra.

4. COMPARISON OF qsGW AND G_0W_0

Given the qsGW results for the IPs from the previous sections, we nextevaluate next how well the traditional G_0W_0 ($G_0W_0$0th) is capable of reproducing them if one employs an improved DFT starting point. One can do so by using parametrized functionals derived from the PBE0 hybrid functional. In addition, the G_0W_0 second order approach[49] ($G_0W_0$2nd), which takes into account off-diagonal elements of Σ in the QP-equation and hence an influence of orbital corrections, is also tested.

4.1. First Ionization Potentials. The HOMO energies obtained from $G_0W_0$0th@PBE (traditional G_0W_0 with a PBE starting point) have a mean absolute error 0.75 eV and show a clear correlation between the error and the actual value. With increasing energy, the error, as compared to qsGW, systematically increases. Employing a PBE0 starting point improves the overall agreement with qsGW down to a mean absolute deviation of 0.42 eV, see Figure 9 and Table 5. Best agreement is achieved employing the PBE-hybrid based starting point
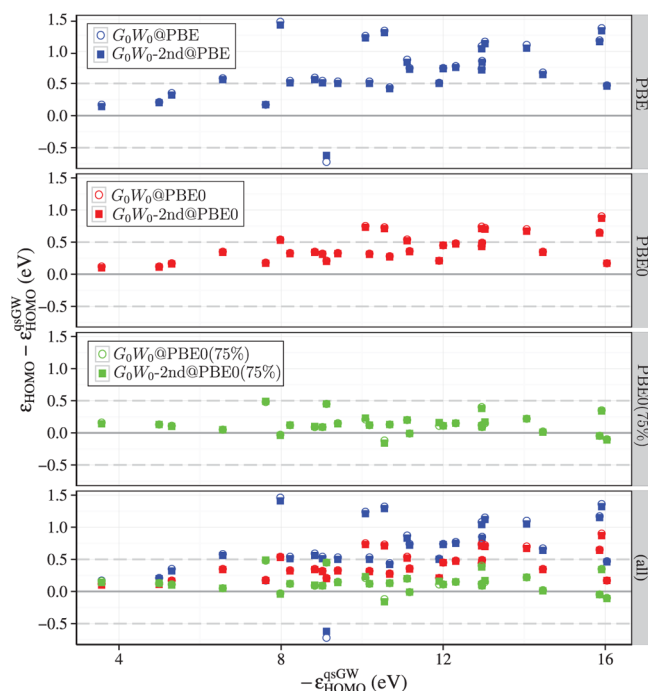
Figure 9. Deviation of HOMO energies obtained from $G_0W_0$0th and $G_0W_0$2nd to qsGW. Results are shown for calculations initialized from DFT, employing PBE and PBE hybrid XC-functionals with an exact exchange contribution of 25% (PBE0) and 75% (PBE0(75%)). On average best agreement is achieved employing the PBE0(75%) starting point, see Table 5.

Table 5. Statistical Measures over the Data from Figure 9[a]

G_0W_0	@PBE		@PBE0		@PBE0(75%)	
	0th	2nd	0th	2nd	0th	2nd
ME	0.70	0.67	0.42	0.41	0.11	0.19
MAE	0.75	0.72	0.42	0.41	0.18	0.26
σ^2	0.20	0.18	0.05	0.04	0.05	0.23
MaxAE	1.46	1.41	0.90	0.87	0.85	2.41
MinAE	0.17	0.14	0.12	0.10	0.01	0.01

[a]Evaluated is the difference of the calculated G_0W_0 and $G_0W_0$2nd HOMO energies to the qsGW HOMO cumulated over the test set. Three different DFT based starting points have been employed. On average, best agreement is achieved with the PBE hybrid XC-functionals with a contribution of exact exchange of 75% as the starting point (PBE0(75%)). All values are in eV.

employing 75% exact exchange. For this starting point, the correlation between the error and ionization energy disappears. Our data also confirms a trend that already appeared in our earlier work: $G_0W_0$0th and $G_0W_0$2th give similar results. This suggests that off-diagonal elements of Σ give negligible contributions to the QP-energies.[49]

4.2. Higher Ionization Potentials. Figure 10 displays the QP-energies from $G_0W_0$0th and $G_0W_0$2th relative to qsGW for different PBE0 based starting points for naphthalene. In our example we find best agreement, with qsGW, employing the starting point with a higher contribution of exchange (PBE0(75%)). Furthermore, we see in the calculation initialized from PBE0(75%) no energy dependent trend in the error, while the trend persists in both $G_0W_0$0th and $G_0W_0$2nd employing a PBE or PBE0 starting point.
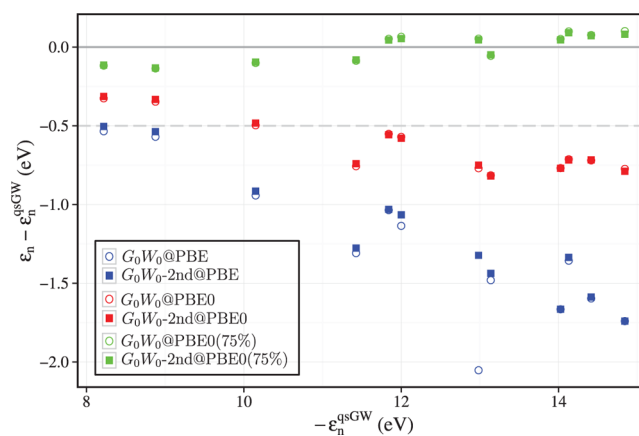
Figure 10. Comparison of the QP-energies from $G_0W_0$0th and $G_0W_0$2nd with qsGW for naphthalene. Three different DFT based starting points employing the PBE and the PBE hybrid functional with 25% (PBE0) and with 75% exact exchange (PBE0(75%)) were chosen. The best agreement, with qsGW, yields the calculation with the PBE0(75%) starting point.

## 5. VALIDATING PARTIAL SELF-CONSISTENCY

Even though computationally more affordable than typical coupled cluster approaches, qsGW is still too expensive for systematic screenings over large ensembles of intermediate sized molecules. Thus, motivated, in this section we test simplified flavors of qsGW. Our aim is to find an approximation scheme that captures the dominant contributions included in qsGW and hence is capable of reproducing results of qsGW, at a lower computational cost.

5.1. qsGW with Fixed Orbitals: evGW. Our studies of the charge density for qsGW suggest that orbital updates tend to be small. Therefore, we next ignore orbital updates in the self-consistency cycle and take into account only the update in the pole positions: eigenvalue only GW (evGW).[26]

5.1.1. Method evGW. Within the methodology described in section 2.1 turning qsGW into evGW is straightforward, one only needs to suppress the update in the orbitals between consecutive qsGW iterations. In other words the machinery operates solely with the initial set of QP-orbitals $\psi^{(0)}(\mathbf{r})$ and the orbital update from eq 13 is skipped. In all equations the orbitals $\psi^{(i)}(\mathbf{r})$ are replaced with $\psi^{(0)}(\mathbf{r})$. Furthermore our treatment of the quasiparticle equation in evGW neglects off-diagonal elements of Σ. Finally we discard the static approximation and restore in the QP-equation the energy-dependent self-energy Σ. Then, for each pole the QP-equation is solved self-consistently. Computationally this introduces the benefit that the Coulomb exchange integrals, see 18, do not need to be re-evaluated. For instance, the full exchange part of the self-energy Σ_x, see 18, needs only one single evaluation.

5.1.2. Comparison to qsGW - First IPs. For the set of molecules specified in Table 1, the differences between the evGW estimates of first IPs and the qsGW results are shown in Figure 11 (see Table 6 for the statistical evaluation). Because evGW is not self-consistent in the orbitals there is a residual starting point dependence, which is clearly visible in Figure 11. It is however significantly reduced as compared to, e.g., G_0W_0. In contrast to the findings from the G_0W_0 before we find best overall agreement with the qsGW by employing the PBE0 functional (and not anymore the PBE0(75%) hybrid with 75% exact exchange). Even for pure PBE the overall agreement with qsGW is better than with PBE0(75%).
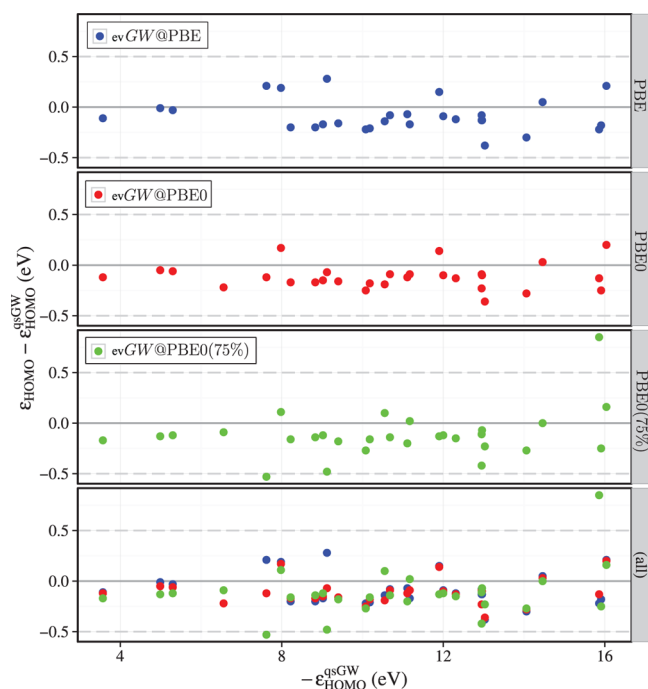
Figure 11. Comparison of HOMO energies using evGW initialized from DFT calculations with the qsGW HOMO energies for the test set. The evGW starting point was constructed from PBE and PBE-hybrid calculations. The results of evGW show only weak dependence on the amount of exact exchange in the functional of the initial DFT calculation.

Table 6. Statistical Evaluation of the Data from Figure 11[a]

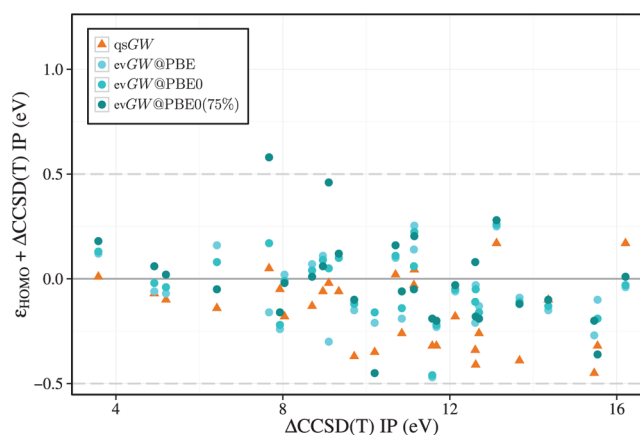| evGW	@PBE	@PBE0	@PBE0(75%)
ME	0.09	0.12	0.12
MAE	0.17	0.15	0.20
σ^2	0.03	0.02	0.06
MaxAE	0.39	0.36	0.85
MinAE	0.01	0.03	0.00

[a]The deviation from calculated evGW HOMO energies (from different PBE and PBE-hybrid starting points) to the qsGW HOMO cumulated over the test set. With evGW we find best agreement with qsGW if the PBE0 starting point is employed. All values are in eV.

5.1.3. Comparison to qsGW - Higher IPs. A comparison of QP-energies from evGW and qsGW is given in Figure 12 for naphthalene. The results confirm the findings for the first IPs. The starting point dependence is strongly reduced, and we find that the trend in the energy dependence of the error, which was present in G_0W_0, is not present anymore for all starting points. All in all, self-consistency in the poles by itself already produces very good agreement with qsGW QP-energies for all starting points.

5.1.4. Comparison to ΔCCSD(T) - First IPs. To further substantiate the accuracy of evGW we present a comparison to ΔCCSD(T)[81] first IPs over the full test set, see Figure 13. The statistical analysis, see Table 7, shows that the overall error is not larger than the error from qsGW. In fact evGW results exhibit an even better agreement with ΔCCSD(T), especially when starting from PBE0. Starting from PBE0(75%), PBE0 with 75% exact exchange introduces various spurious outliers. Summarizing, evGW seems to be a promising alternative to qsGW leading in practice to results very close to the
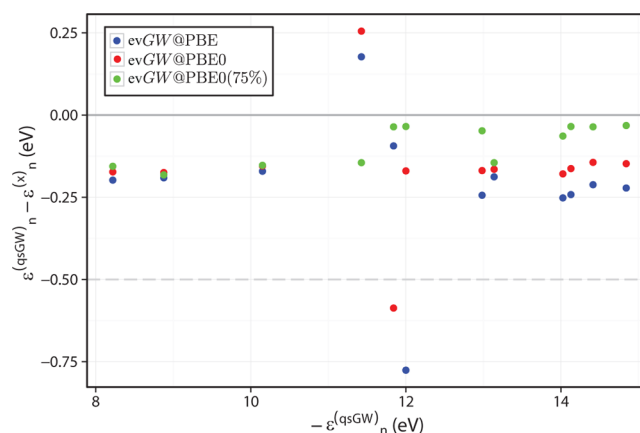
Figure 12. Deviation of the QP-energies from evGW from different PBE and PBE-hybrid starting points to qsGW for naphthalene.

Figure 13. Comparison of the HOMO energies using evGW initialized from different DFT(PBEλ) starting points and qsGW calculations to the ΔCCSD(T)[81] IP energies.

Table 7. Statistical Evaluation of the Data Shown in Figure 13[a]

		evGW		
	qsGW	@PBE	@PBE0	@PBE0(75%)
ME	−0.16	−0.07	−0.04	−0.04
MAE	0.19	0.15	0.12	0.18
σ^2	0.02	0.01	0.01	0.06
MaxAE	0.45	0.47	0.46	1.17
MinAE	0.01	0.02	0.01	0.01

[a]The evGW approach shows better agreement with the ΔCCSD(T) reference than the qsGW approach, for all considered starting points. Best agreement of evGW with ΔCCSD(T) is achieved by employing the PBE0 functional in the starting point for the DFT calculation. All values are in eV.

ΔCCSD(T) reference, with a typical deviation of a few 100 meV.

5.2. Comparison of $G_{ev}W_0$ versus qsGW. So far, our results indicated that orbital updates have a minor effect on the pole positions of qsGW. The next question is whether the QP-energies are as sensitive to the pole positions of W as they are to the pole positions of G in Σ. To this end we recall an approximate scheme, $G_{ev}W_0$, which we introduced before.[49] It keeps the screened interaction based on the starting point calculation W_0 and introduces self-consistency only at the pole

positions of the Green's function. The computational cost of $G_{ev}W_0$ is the same as traditional G_0W_0 (within our implementation).

5.2.1. First Ionization Potentials. Figure 14 shows the difference of the HOMO energy obtained as from $G_{ev}W_0$ to the
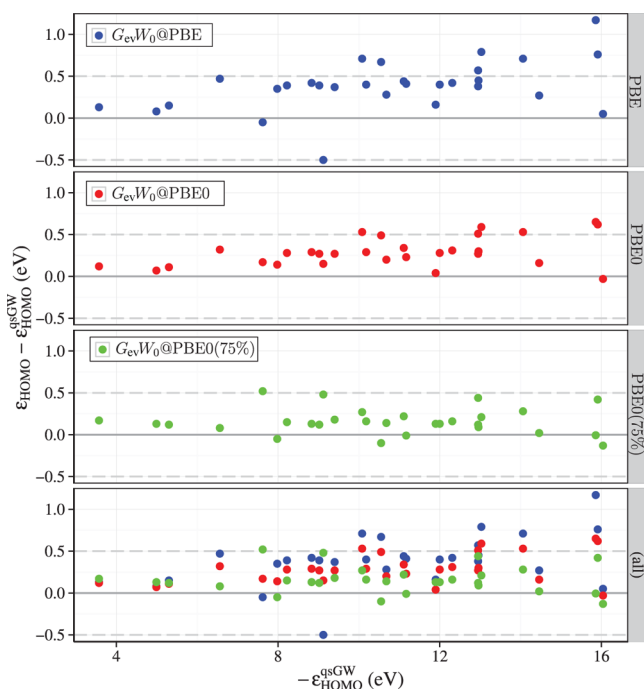
Figure 14. Difference of calculated HOMO energies using $G_{ev}W_0$ to DFT(PBEλ) starting points to the qsGW HOMO energies. With increasing exact exchange contribution in the PBEλ starting point improves the agreement with qsGW. Nevertheless, we find for all starting points an error which increases with energy. The statistical evaluation is reported in Table 8.

qsGW HOMO energies for the full test set. The statistical measures are reported in Table 8. The first IPs from $G_{ev}W_0$

Table 8. Statistical Measures of the Difference of the Calculated $G_{ev}W_0$ HOMO Energies from DFT(PBEλ) Starting Points to the qsGW HOMO Accumulated over the Test Set[a]

| $G_{ev}W_0$	@PBE	@PBE0	@PBE0(75%)
ME	0.39	0.29	0.13
MAE	0.43	0.30	0.21
σ^2	0.09	0.03	0.06
MaxAE	1.18	0.66	0.83
MinAE	0.04	0.04	0.01

[a]Best agreement is achieved employing the PBE0(75%) starting point. All values are in eV.

show a reduced starting point dependence in comparison to the single-shot G_0W_0 and the $G_0W_0$2nd results. However, the starting point dependence is much stronger than in the case of evGW. Furthermore, $G_{ev}W_0$ shows improved agreement with qsGW if one employs the PBE or PBE0 starting point. If one employs the optimal PBE0(75%) starting points the plain G_0W_0 and the $G_{ev}W_0$ are comparable close to the qsGW results.

Comparing the optimal staring point we find for the three different approximate GW flavors, G_0W_0, evGW, and $G_{ev}W_0$, there are some interesting remarks to make. In evGW the

differences are rather small with a small preference of PBE0, which is in agreement with PBE0 having the best dipole moment of the various starting points. The results are comparable to those of qsGW. The exact shape of the orbitals hence does not impact the results that much. However, if W is kept fixed there is a clear preference for a PBE0(75%) starting point. This indicates that, given the relatively small spread in orbitals obtained in the range from PBE to HF, it is primarily important to have an accurate screening. The quality of the orbitals is only of secondary importance. This is also reflected in the small orbital corrections obtained in qsGW.

5.2.2. Higher Ionization Potentials. In Figure 15 the QP-energies from $G_{ev}W_0$ are compared to the ones from qsGW for
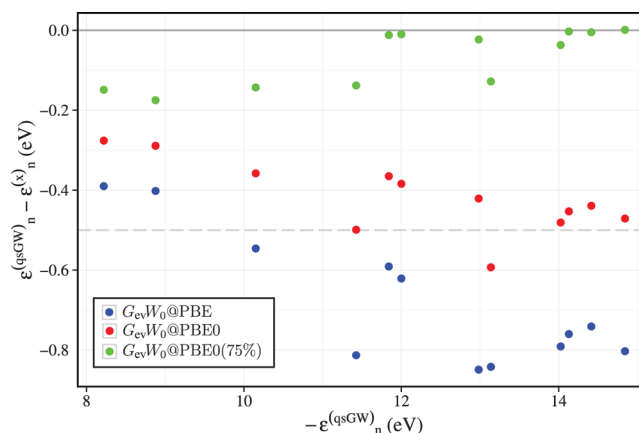

Figure 15. Deviation of the QP-energies from $G_{ev}W_0$ to QP-energies from qsGW for naphthalene. Three different DFT based starting points employing the PBE and the PBE hybrid functional with 25% (PBE0) and with 75% exact exchange (PBE0(75%)) were chosen. The best agreement, with qsGW, yields the calculation with the PBE0(75%) starting point.

naphthalene. The spectrum based on $G_{ev}W_0$ shows a slight overestimation of the QP-energies for all starting points. Furthermore, we find that the shift on the poles from the self-energy due to the QP-correction corrects to poles toward the full qsGW solution. Regarding the starting point dependence we find again that the PBE0(75%) gives best agreement with the qsGW results.

6. COMPUTATIONAL PERFORMANCE

The total computational effort needed for one GW iteration comprises the calculation of the response function and the self-energy part. Under the latter we understand the construction of the self-energy and the solution of the quasi-particle equation. The time needed for the construction of the response function is for all considered approximations identical. The time needed for the self-energy part varies depending on the treatment of the QP-equation. Figure 16 displays the computational cost for the different (approximate) GW flavors within our implementation.

The $G_0W_0$0th approach is by far the fastest and shows the best scaling with the number of basis functions of only $\sim N^3$ for the self-energy part. The computational cost for $G_0W_0$0th calculations are hence dominated by the construction of the response function, which has a scaling of $\sim N^4$. However, this is only true for comparably small molecules. In the exact evaluation, one has to calculate all excitations, and a matrix of range $\sim N^2$ has to be diagonalized. This is a hard $\sim N^6$-step but
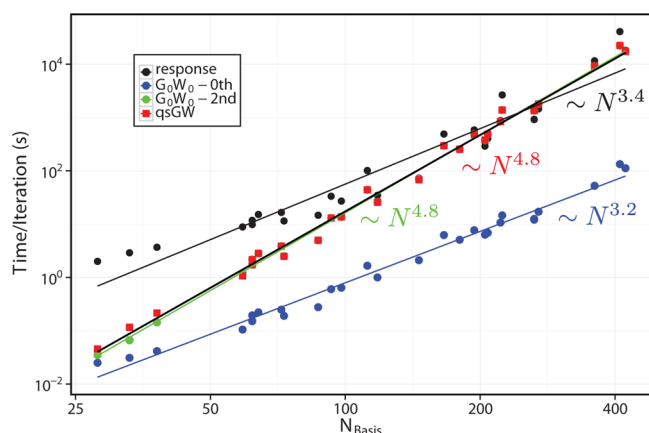
Figure 16. Computational time needed for the construction of the response function and the time needed for a single iteration GW-proper over the number of basis functions. In evGW every full iteration consists of a response step and a $G_0W_0$0th step. In $G_{ev}W_0$ only the first iteration has a response step, subsequent steps are computationally equivalent to a $G_0W_0$0th step, and times are almost the same for both procedures.

with a small prefactor and still less than a $\sim N^7$ scaling for CCSD(T) in conventional implementations.

Similar to G_0W_0, evGW approach operates solely on the diagonal part of the QP-equation. Hence, it has the same scaling behavior as (diagonal only) $G_0W_0$0th, but, to find a self-consistent solution, typically six iterations are necessary until convergence is achieved. Hence, the total time needed for evGW is that of G_0W_0 plus six times that of the response calculation.

Both, with $G_0W_0$2nd and the qsGW approach, which diagonalize the quasi-particle equation (eq 10), the self-energy part shows a scaling with the number of basis functions N of $\sim N^5$, worse by a factor of N^2 as compared to $G_0W_0$0th and evG_0W_0. Still we find that the computational time needed for the majority of the molecules within our test set is dominated by the construction of the response function. Only for systems requiring more than 340 basis functions, the self-energy part begins to dominate the computational cost. An actual optimization for best performance within the GW is still an open task within our implementation. Especially in the qsGW implementation we expect room for improvement.

Note that all self-energy parts of our implementation have been designed for parallel computation. We find for all approaches a nearly perfect scaling with the number of cores, i.e. the typical setup of 8 core nodes gives a typical speedup of 7.94. Hence, due to very good parallel scaling larger scale systems are tractable.

7. SUMMARY

Considering the first IPs, we confirm for a set of 29 representative molecules that all flavors of the GW method strongly improve agreement with experiment and CCSD(T) results as compared to the underlying DFT calculation. Moreover, the self-consistent qsGW improves agreement with the CCSD(T) by an order of magnitude as compared to $G_0W_0$0th using a semilocal starting point (see Figure 5). Also, we find that qsGW has a better agreement with experiment in ionization spectra as compared to results based on G_0W_0 using a semilocal starting point by typically 500 meV. Using an optional staring point, i.e. PBE0(75%) for G_0W_0 and $G_{ev}W_0$ and

PBE0 for evGW, gives results very close to qsGW. Comparing qsGW and scGW, we observed a rigid shift toward stronger binding in qsGW, in the favor of qsGW for both dipole moments and ionization energies. The small number of molecules however prohibits to make a final claim on the ultimate accuracy difference between sc and qsGW for molecules. A study comparing the two using the GW100 set[48] is currently under way.

The qsGW introduces only minor corrections on the spatial shape of the QP-orbitals and ground state density as compared to the KS-reference. Comparing calculated dipole moments to experimental results we find that the qsGW improves agreement to experiment compared to a traditional method like the Density Functional Theory (DFT) using a PBE functional and the Hartree−Fock (HF) approach (see Table 4).

Based on this result we conclude that for the partially self-consistent flavor of qsGW updating only the orbitals, eigenvalue only qsGW (evGW) is an efficient alternative. The evGW is able to reproduce the (first) IPs from qsGW very well and showed a strongly reduced dependence on the choice of the functional in comparison to G_0W_0.

If system size is prohibiting even evGW we find the best alternative to be G_0W_0@PBE0(75%). The increased amount of exact exchange is reasoned to mainly be necessary to improve the screening. Since the standard PBE0 orbitals turn out to be in general closest to the qsGW results and also give best dipole moments as compared to experiment, one could even envision a hybrid approach. This would use the orbitals from PBE0 but perturbatively correct the eigenvalues using 75% exact exchange before calculating the response function.

8. OUTLOOK

The full solution of Hedin's equations gives access not only to the quasi-particle (qp) energies but also to charge neutral, particle-hole (ph) type excitations. A characteristic feature that all variants of the GW theory share is that the energy of a ph-excitation is estimated neglecting the interaction between the particle and the hole, so that there is a tendency to overestimate the energy cost for creating ph-pairs, i.e. excitons.[98] As a result the Coulomb interaction is underscreened, which leads to an underestimation of the magnitude of the correlation part of the self-energy. Thus, the HOMO energy is typically under-estimated (i.e., the ionization potential is overestimated) as also observed in our results.

There is no real consensus about the consequences of underscreening for the qp-energies. A widespread belief is that underscreening in the effective interaction W (denominator) does not affect these energies, because it is fully canceled by the explicit vertex corrections (Γ, nominator) appearing in the self-energy diagrams. Rigorous arguments in favor of the cancellation have not been given; so far, the existing evidence supporting cancellation relies on explicit calculations for a number of test systems, such as, e.g., homogeneous electron gases[99] and bulk silicon.[100]

Our results indicate that when applying qsGW to single molecules, HOMO energies and ionization potentials are typically underestimated. In our opinion, a natural explanation is underscreening of the Coulomb-interaction in W; we hence propose that the cancellation of vertex-terms is not efficient in molecular matter.

To account for the binding-energy of excitons in the polarization function, one has to go beyond the GW-framework, i.e., include vertex corrections. A common means

to this end is solving the Bethe-Salpeter equation (BSE).[101] This is computationally challenging, however, and can be done only by employing suitable approximation schemes.[102]

On the simplest level (RPA-X) one modifies the calculation of the polarization function by adding an exchange-matrix element to the Coulomb-matrix element of conventional RPA. The resulting theory would reproduce the time-dependent Hartree−Fock approximation if it were not for the correlation part of the self-energy. Following our philosophy of exploring the potential of static approximations, this step would be the most natural one to try next for us.

Indeed, several groups have already employed the GW+BSE method to molecular systems in order to investigate the effect of vertex corrections for charge-neutral excitations. We only mention two very recent works benchmarking the approach against TDDFT for small molecules.[103,104] We would like to consider these results as an indication that vertex-corrections are indeed significant for predicting and understanding molecular spectra. These studies also indicate that BSE-calculations inherit the starting point dependency of the underlying G_0W_0-calculations.[103] To eliminate this artifact of G_0W_0, self-consistent calculations on the qsGW-level have been employed; they can achieve a numerical accuracy comparable to TD-PBE0 calculations.[104]

As promising as it is, the combination of GW and BSE adds vertex corrections only to the response function still neglecting them when constructing Γ for the self-energy Σ. The approximation thus obtained is not conserving. Moreover, if indeed large system classes exhibit a cancellation between vertex terms in W and Γ, then these systems cannot be treated with the present technology. Therefore, we consider it very likely that a general method to be applied successfully to molecules and metals has to treat vertex corrections in W and Σ on the same footing.

In principle, also the study of strongly correlated electron liquids relies on solving Hedin's equations—at least to the extent that perturbative methods are being employed—even though the respective community does not usually think about it in this way. In this context, a new method has been devised in recent years, the *functional renormalization group* method (FRG)[105,106] Unlike GW+BSE, FRG includes vertex corrections to W and Σ in a consistent way. Its success for strongly correlated matter originates from its capability to reliably signalize the existence of new phases with a broken symmetry, such as magnetism. From a conceptual point of view, FRG is very appealing because it can predict phase transitions in an unbiased manner; in principle, an *apriori* guess about what phases are likely to appear is not required.

Similar to qsGW, also FRG is typically formulated employing a static approximation for the self-energy and the interaction vertex. Like traditional BSE-calculations, also the FRG focuses on the simplest subset of diagrams for the vertex. However, in contrast to traditional BSE, the FRG solves these (approximated) Hedin equations in a self-consistent manner. This is how FRG goes beyond the GW+BSE-scheme.

The enhanced complexity requires a solution strategy that differs from the conventional iteration scheme to self-consistency still underlying, e.g., qsGW. The strategy of FRG is to reformulate the self-consistency problem in terms of a set of (nonlinear) differential matrix equations. The main idea may be understood as follows: In traditional self-consistency solvers, an initial guess gradually transforms ("flows") into the fixed-point solution under the action of the iteration routine. Now,

FRG replaces this "iterative flow" by another flow along an artificial coordinate, Λ, that plays the role of a cutoff energy familiar from the renormalization group. By construction, Λ connects a known trivial solution of Hedin's equations at $\Lambda = \infty$ with the exact solution at $\Lambda = 0$. The advantage of this formulation as compared to the traditional self-consistency routines is that it is known exactly how to initialize the flow equations; a starting guess for the Green's function, self-energy and interaction vertex is not required. If instabilities occur along solving the differential equation, then these can be interpreted as "runaway flow" indicating a nearby phase with broken symmetry.

Applications of FRG to molecules do not yet exist. A first step into this direction has been made recently by two of us who formulated the FRG for systems without translational invariance.[107] Since vertex functions are kept explicitly, FRG comes with a computational complexity that might prohibit its use for intermediate sized molecular systems in the near future. Nevertheless, for benchmarking GW+BSE and high precision calculations for smaller molecules, FRG could have a significant potential that we believe is worthwhile to explore in future research.

■ ASSOCIATED CONTENT

⑤ Supporting Information

The Supporting Information is available free of charge on the ACS Publications website at DOI: 10.1021/acs.jctc.5b01238.

> Full details of the used atomic structures (TXT)
> Tables containing the calculated I_P's and E_A's as well as analysis of the computational performance and scaling scaling behavior of the competing methods (PDF)

■ AUTHOR INFORMATION

Corresponding Author
*E-mail: mjvansetten@gmail.com.
Notes
The authors declare no competing financial interest.

■ ACKNOWLEDGMENTS

■ REFERENCES

(1) Kohn, W. *Rev. Mod. Phys.* **1999**, 71, 1253.
(2) Kohn, W.; Sham, L. J. *Phys. Rev.* **1965**, 140, A1133.
(3) Chong, D.; Gritsenko, O.; Baerends, E. *J. Chem. Phys.* **2002**, 116, 1760−1772.
(4) Gritsenko, O.; Baerends, E. J. *Can. J. Chem.* **2009**, 87, 1383−1391.

(5) Baerends, E. J.; Gritsenko, O. V.; van Meer, R. *Phys. Chem. Chem. Phys.* **2013**, *15*, 16408−16425.

(6) Hedin, L. *Phys. Rev.* **1965**, *139*, A796.

(7) Hedin, L. *Ark. Fys.* **1965**, *30*, 231.

(8) Hedin, L.; Lundqvist, B. I. *J. Phys. C: Solid State Phys.* **1971**, *4*, 2064.

(9) Hedin, L. *J. Phys.: Condens. Matter* **1999**, *11*, R489.

(10) Abrikosov, A. A.; Gorkov, L. P.; Džalošinskij, I. E. *Methods of quantum field theory in statistical physics*; Doverice-Hall: 1963; pp 51−77.

(11) Fetter, A. L.; Walecka, J. D. *Quantum theory of many-particle systems*; Dover Publ.: 1971; pp 53−100.

(12) Ethridge, E. C.; Fry, J. L.; Zaider, M. *Phys. Rev. B: Condens. Matter Mater. Phys.* **1996**, *53*, 3662−3668.

(13) Ishii, S.; Ohno, K.; Kawazoe, Y.; Louie, S. G. *Phys. Rev. B: Condens. Matter Mater. Phys.* **2001**, *63*, 155104.

(14) Grossman, J. C.; Rohlfing, M.; Mitas, L.; Louie, S. G.; Cohen, M. L. *Phys. Rev. Lett.* **2001**, *86*, 472.

(15) Ishii, S.; Ohno, K.; Kawazoe, Y.; Louie, S. G. *Phys. Rev. B: Condens. Matter Mater. Phys.* **2002**, *65*, 245109.

(16) Ismail-Beigi, S.; Louie, S. G. *Phys. Rev. Lett.* **2003**, *90*, 076401.

(17) Pavlyukh, Y.; Hübner, W. *Phys. Lett. A* **2004**, *327*, 241.

(18) Tiago, M. L.; Chelikowsky, J. R. *Phys. Rev. B: Condens. Matter Mater. Phys.* **2006**, *73*, 205334.

(19) Lopez del Puerto, M. L.; Tiago, M. L.; Chelikowsky, J. R. *Phys. Rev. Lett.* **2006**, *97*, 096401.

(20) Lopez del Puerto, M. L.; Tiago, M. L.; Chelikowsky, J. R. *Phys. Rev. B: Condens. Matter Mater. Phys.* **2008**, *77*, 045404.

(21) Ramos, L. E.; Paier, J.; Kresse, G.; Bechstedt, F. *Phys. Rev. B: Condens. Matter Mater. Phys.* **2008**, *78*, 195423.

(22) Noguchi, Y.; Ishii, S.; Ohno, K.; Sasaki, T. *J. Chem. Phys.* **2008**, *129*, 104104.

(23) Bruneval, F. *Phys. Rev. Lett.* **2009**, *103*, 176403.

(24) Tiago, M. L.; Idrobo, J. C.; Öğüt, S.; Jellinek, J.; Chelikowsky, J. R. *Phys. Rev. B: Condens. Matter Mater. Phys.* **2009**, *79*, 155419.

(25) Rostgaard, C.; Jacobsen, K. W.; Thygesen, K. S. *Phys. Rev. B: Condens. Matter Mater. Phys.* **2010**, *81*, 085103.

(26) Blase, X.; Attaccalite, C.; Olevano, V. *Phys. Rev. B: Condens. Matter Mater. Phys.* **2011**, *83*, 115103.

(27) Qian, X.; Umari, P.; Marzari, N. *Phys. Rev. B: Condens. Matter Mater. Phys.* **2011**, *84*, 075103.

(28) Refaely-Abramson, S.; Baer, R.; Kronik, L. *Phys. Rev. B: Condens. Matter Mater. Phys.* **2011**, *84*, 075144.

(29) Foerster, D.; Koval, P.; Sanchez-Portal, D. *J. Chem. Phys.* **2011**, *135*, 074105.

(30) Ke, S. *Phys. Rev. B: Condens. Matter Mater. Phys.* **2011**, *84*, 205415.

(31) Baumeier, B.; Andrienko, D.; Ma, Y.; Rohlfing, M. *J. Chem. Theory Comput.* **2012**, *8*, 997.

(32) Sharifzadeh, S.; Tamblyn, I.; Doak, P.; Darancet, P. T.; Neaton, J. B. *Eur. Phys. J. B* **2012**, *85*, 323.

(33) Nguyen, H.-V.; Pham, T. A.; Rocca, D.; Galli, G. *Phys. Rev. B: Condens. Matter Mater. Phys.* **2012**, *85*, 081101.

(34) Ren, X.; Rinke, P.; Blum, V.; Wieferink, J.; Tkatchenko, A.; Sanfilippo, A.; Reuter, K.; Scheffler, M. *New J. Phys.* **2012**, *14*, 053020.

(35) Hübener, H.; Pérez-Osorio, M. A.; Ordejón, P.; Giustino, F. *Phys. Rev. B: Condens. Matter Mater. Phys.* **2012**, *85*, 245125.

(36) Bruneval, F. *J. Chem. Phys.* **2012**, *136*, 194107.

(37) Pham, T. A.; Nguyen, H.-V.; Rocca, D.; Galli, G. *Phys. Rev. B: Condens. Matter Mater. Phys.* **2013**, *87*, 155148.

(38) Bruneval, F.; Marques, M. A. L. *J. Chem. Theory Comput.* **2013**, *9*, 324.

(39) Faber, C.; Attaccalite, C.; Olevano, V.; Runge, E.; Blase, X. *Phys. Rev. B: Condens. Matter Mater. Phys.* **2011**, *83*, 115123.

(40) van Setten, M. J.; Weigend, F.; Evers, F. *J. Chem. Theory Comput.* **2013**, *9*, 232−246.

(41) Faber, C.; Boulanger, P.; Attaccalite, C.; Duchemin, I.; Blase, X. *Philos. Trans. R. Soc., A* **2014**, *372*, 20130271.

(42) Faber, C.; Boulanger, P.; Duchemin, I.; Attaccalite, C.; Blase, X. *J. Chem. Phys.* **2013**, *139*, 194308.

(43) Baumeier, B.; Rohlfing, M.; Andrienko, D. *J. Chem. Theory Comput.* **2014**, *10*, 3104−3110.

(44) Ren, X.; Marom, N.; Caruso, F.; Scheffler, M.; Rinke, P. *Phys. Rev. B: Condens. Matter Mater. Phys.* **2015**, *92*, 081104.

(45) Migani, A.; Mowbray, D. J.; Zhao, J.; Petek, H. *J. Chem. Theory Comput.* **2015**, *11*, 239−251.

(46) Laflamme Janssen, J.; Rousseau, B.; Cote, M. *Phys. Rev. B: Condens. Matter Mater. Phys.* **2015**, *91*, 125120.

(47) Kühn, M.; Weigend, F. *J. Chem. Theory Comput.* **2015**, *11*, 969−979.

(48) van Setten, M. J.; Caruso, F.; Sharifzadeh, S.; Ren, X.; Scheffler, M.; Liu, F.; Lischner, J.; Lin, L.; Deslippe, J. R.; Louie, S. G.; Yang, C.; Weigend, F.; Neaton, J. B.; Evers, F.; Rinke, P. *J. Chem. Theory Comput.* **2015**, *11*, 5665−5687.

(49) Kaplan, F.; Weigend, F.; Evers, F.; van Setten, M. J. *J. Chem. Theory Comput.* **2015**, *11*, 5152−5160.

(50) Gallandi, L.; Körzdörfer, T. *J. Chem. Theory Comput.* **2015**, *11*, 5391−5400.

(51) Wang, L.-W. *Phys. Rev. B: Condens. Matter Mater. Phys.* **2015**, *91*, 125135.

(52) Caruso, F.; Rinke, P.; Ren, X.; Scheffler, M.; Rubio, A. *Phys. Rev. B: Condens. Matter Mater. Phys.* **2012**, *86*, 081102.

(53) Kaasbjerg, K.; Thygesen, K. S. *Phys. Rev. B: Condens. Matter Mater. Phys.* **2010**, *81*, 085102.

(54) Sakuma, R.; Miyake, T.; Aryasetiawan, F. *Phys. Rev. B: Condens. Matter Mater. Phys.* **2009**, *80*, 235128.

(55) Stan, A.; Dahlen, N. E.; van Leeuwen, R. *J. Chem. Phys.* **2009**, *130*, 114105.

(56) Holm, B.; von Barth, U. *Phys. Rev. B: Condens. Matter Mater. Phys.* **1998**, *57*, 2108−2117.

(57) Caruso, F.; Rinke, P.; Ren, X.; Rubio, A.; Scheffler, M. *Phys. Rev. B: Condens. Matter Mater. Phys.* **2013**, *88*, 075105.

(58) Gatti, M.; Bruneval, F.; Olevano, V.; Reining, L. *Phys. Rev. Lett.* **2007**, *99*, 266402.

(59) Koval, P.; Foerster, D.; Sanchez-Portal, D. *Phys. Rev. B: Condens. Matter Mater. Phys.* **2014**, *89*, 155417.

(60) van Schilfgaarde, M.; Kotani, T.; Faleev, S. *Phys. Rev. Lett.* **2006**, *96*, 226402.

(61) Faleev, S. V.; van Schilfgaarde, M.; Kotani, T. *Phys. Rev. Lett.* **2004**, *93*, 126406.

(62) van Schilfgaarde, M.; Kotani, T.; Faleev, S. *Phys. Rev. Lett.* **2006**, *96*, 226402.

(63) Kotani, T.; Van Schilfgaarde, M.; Faleev, S. V. *Phys. Rev. B: Condens. Matter Mater. Phys.* **2007**, *76*, 1−24.

(64) Shishkin, M.; Kresse, G. *Phys. Rev. B: Condens. Matter Mater. Phys.* **2007**, *75*, 235102.

(65) Shishkin, M.; Marsman, M.; Kresse, G. *Phys. Rev. Lett.* **2007**, *99*, 246403.

(66) Bruneval, F.; Vast, N.; Reining, L. *Phys. Rev. B: Condens. Matter Mater. Phys.* **2006**, *74*, 045102.

(67) Bruneval, F.; Vast, N.; Reining, L.; Izquierdo, M.; Sirotti, F.; Barrett, N. *Phys. Rev. Lett.* **2006**, *97*, 267601.

(68) Holm, B.; von Barth, U. *Phys. Scr.* **2004**, *2004*, 135.

(69) Rinke, P.; Qteish, A.; Neugebauer, J.; Freysoldt, C.; Scheffler, M. *New J. Phys.* **2005**, *7*, 126.

(70) Fuchs, F.; Furthmüller, J.; Bechstedt, F.; Shishkin, M.; Kresse, G. *Phys. Rev. B: Condens. Matter Mater. Phys.* **2007**, *76*, 115109.

(71) Körzdörfer, T.; Marom, N. *Phys. Rev. B: Condens. Matter Mater. Phys.* **2012**, *86*, 041110.

(72) Marom, N.; Caruso, F.; Ren, X.; Hofmann, O. T.; Körzdörfer, T.; Chelikowsky, J. R.; Rubio, A.; Scheffler, M.; Rinke, P. *Phys. Rev. B: Condens. Matter Mater. Phys.* **2012**, *86*, 245127.

(73) Atalla, V.; Yoon, M.; Caruso, F.; Rinke, P.; Scheffler, M. *Phys. Rev. B: Condens. Matter Mater. Phys.* **2013**, *88*, 165122.

(74) Körzdörfer, T.; Marom, N. *Phys. Rev. B: Condens. Matter Mater. Phys.* **2012**, *86*, 041110.

(75) Lischner, J.; Sharifzadeh, S.; Deslippe, J.; Neaton, J. B.; Louie, S. G. *Phys. Rev. B: Condens. Matter Mater. Phys.* **2014**, *90*, 115130.

(76) Fuchs, F.; Furthmüller, J.; Bechstedt, F.; Shishkin, M.; Kresse, G. *Phys. Rev. B: Condens. Matter Mater. Phys.* **2007**, *76*, 115109.

(77) Shishkin, M.; Marsman, M.; Kresse, G. *Phys. Rev. Lett.* **2007**, *99*, 246403.

(78) Gonze, X.; Rignanese, G.-M.; Verstraete, M.; Beuken, J.-M.; Pouillon, Y.; Caracas, R.; Jollet, F.; Torrent, M.; Zerah, G.; Mikami, M.; Ghosez, P.; Veithen, M.; Raty, J.-Y.; Olevano, V.; Bruneval, F.; Reining, L.; Godby, R.; Onida, G.; Hamann, D.; Allan, D. Z. *Kristallogr. - Cryst. Mater.* **2005**, *220*, 558−562.

(79) Purvis, G. D., III; Bartlett, R. J. *J. Chem. Phys.* **1982**, *76*, 1910.

(80) Raghavachari, K.; Trucks, G. W.; Pople, J. A.; Head-Gordon, M. *Chem. Phys. Lett.* **1989**, *157*, 479.

(81) Krause, K.; Harding, M. E.; Klopper, W. *Mol. Phys.* **2015**, *113*, 1952−1960.

(82) Sakuma, R.; Miyake, T.; Aryasetiawan, F. *Phys. Rev. B: Condens. Matter Mater. Phys.* **2009**, *80*, 235128.

(83) Weigend, F.; Ahlrichs, R. *Phys. Chem. Chem. Phys.* **2005**, *7*, 3297.

(84) Weigend, F. *Phys. Chem. Chem. Phys.* **2006**, *8*, 1057.

(85) Tandetzky, F.; Dewhurst, J. K.; Sharma, S.; Gross, E. K. U. *Phys. Rev. B: Condens. Matter Mater. Phys.* **2015**, *92*, 115125.

(86) Perdew, J. P.; Wang, Y. *Phys. Rev. B: Condens. Matter Mater. Phys.* **1992**, *45*, 13244.

(87) Perdew, J. P.; Burke, K.; Ernzerhof, M. *Phys. Rev. Lett.* **1996**, *77*, 3865.

(88) Perdew, J. P.; Ernzerhof, M.; Burke, K. *J. Chem. Phys.* **1996**, *105*, 9982.

(89) The set of molecules used in this manuscript is based on the GW27 set excluding anthracene and naphthacene and adds thiophene, benzothiazole, 1,2,5-thiadiazole, and tetrathiofulvalene. These four are added to compare to existing full self-consistent GW results.

(90) Mayer, P. M.; Blanchet, V.; Joblin, C. *J. Chem. Phys.* **2011**, *134*, 244312.

(91) Holm, B.; von Barth, U. *Phys. Rev. B: Condens. Matter Mater. Phys.* **1998**, *57*, 2108.

(92) In Koval et al. 'B' method the off-diagonal matrix elements of the self-energy are approximated by evaluating them at the Fermi energy. Koval et al. observe convergence problems in the 'A' method and report the main results obtained in the 'B' method. In our implementation, using the linear mixing scheme as described in section 2.2.2, we have no convergence problems. Koval et al. also report a nonmonotonous convergence with respect to the basis-set in the 'A'-method. We observe this as well but only for some very small molecules (hydrogen and nitrogen).

(93) Dunning, T. H. *J. Chem. Phys.* **1989**, *90*, 1007−1023.

(94) Nelson, W.; Bokes, P.; Rinke, P.; Godby, R. W. *Phys. Rev. A: At., Mol., Opt. Phys.* **2007**, *75*, 032505.

(95) Aryasetiawan, F.; Sakuma, R.; Karlsson, K. *Phys. Rev. B: Condens. Matter Mater. Phys.* **2012**, *85*, 035106.

(96) Caruso, F.; Atalla, V.; Ren, X.; Rubio, A.; Scheffler, M.; Rinke, P. *Phys. Rev. B: Condens. Matter Mater. Phys.* **2014**, *90*, 085141.

(97) http://cccbdb.nist.gov (accessed 22-04-2016).

(98) The situation is analogous in time dependent density functional theory when adiabatic approximations are being employed.

(99) Mahan, G. D.; Sernelius, B. E. *Phys. Rev. Lett.* **1989**, *62*, 2718−2720.

(100) Del Sole, R.; Reining, L.; Godby, R. W. *Phys. Rev. B: Condens. Matter Mater. Phys.* **1994**, *49*, 8024−8028.

(101) Giuliani, G.; Vignale, G. *Quantum Theory of the Electron Liquid*; Cambridge University Press: 2008; p 309.

(102) Sander, T.; Maggio, E.; Kresse, G. *Phys. Rev. B: Condens. Matter Mater. Phys.* **2015**, *92*, 045209.

(103) Bruneval, F.; Hamed, S. M.; Neaton, J. B. *J. Chem. Phys.* **2015**, *142*, 244101.

(104) Jacquemin, D.; Duchemin, I.; Blase, X. *J. Chem. Theory Comput.* **2015**, *11*, 3290.

(105) Salmhofer, M. *Renormalization: An Introduction*; Springer: Berlin, Heidelberg, 1999.

(106) Metzner, W.; Salmhofer, M.; Honerkamp, C.; Meden, V.; Schoenhammer, K. *Rev. Mod. Phys.* **2012**, *84*, 299.

(107) Seiler, C.; Evers, F. 2016, arXiv:1605.07024.